



Spectral calibration of SNDICE

E Barrelet, C Juramy, K Schahmaneche

► **To cite this version:**

E Barrelet, C Juramy, K Schahmaneche. Spectral calibration of SNDICE. [Research Report] 2009-01, Laboratoire de Physique Nucléaire et de Hautes Énergies. 2009. <hal-01267313>

HAL Id: hal-01267313

<http://hal.upmc.fr/hal-01267313>

Submitted on 4 Feb 2016

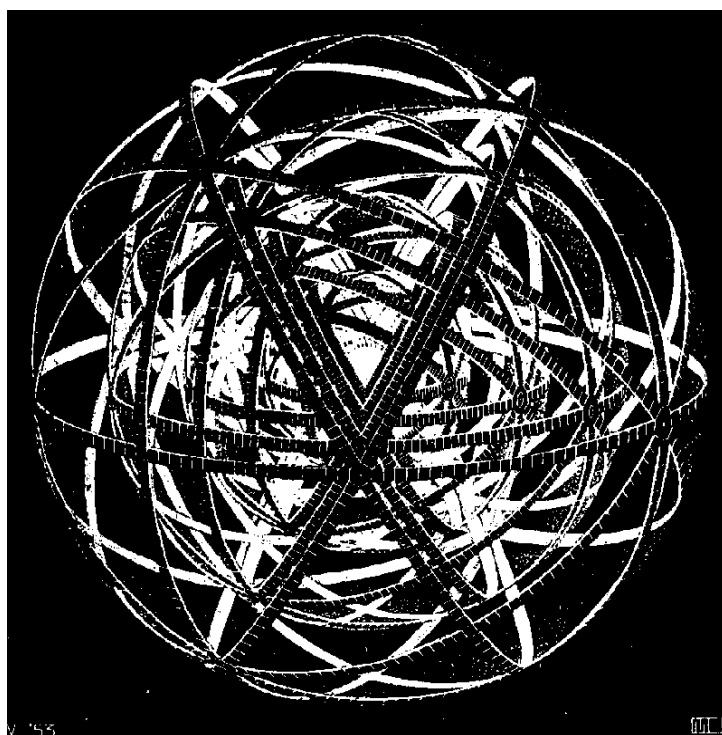
HAL is a multi-disciplinary open access archive for the deposit and dissemination of scientific research documents, whether they are published or not. The documents may come from teaching and research institutions in France or abroad, or from public or private research centers.

L'archive ouverte pluridisciplinaire **HAL**, est destinée au dépôt et à la diffusion de documents scientifiques de niveau recherche, publiés ou non, émanant des établissements d'enseignement et de recherche français ou étrangers, des laboratoires publics ou privés.

Laboratoire de Physique Nucléaire et de Hautes Énergies
CNRS - IN2P3 - Universités Paris VI et VII

Spectral calibration of SNDICE

E. Barrelet, C. Juramy, K. Schahmaneche



4, Place Jussieu - Tour 33 - Rez-de-Chaussée
75252 Paris Cedex 05
Tél.: 33(1) 44 27 63 13 - FAX: 33(1) 44 27 46 38

1 Introduction

SNDICE primary goal was to provide a photometric calibration of the CFH telescope in order to supplement its astronomic calibration based on reference stars. In particular it is intended to uniformize the response of the telescope over the very large field of the Megacam instrument and over well defined segments of the optical spectrum corresponding more or less to the filter set used for the SNLS experiment. The study of spectral features of the LED sources used by SNDICE came in this perspective mainly as a way to quantify second order corrections taking into account the shape of the spectral distribution around its central wavelength value. The spectrophotometric bench presented here did not need to have a precision better than a few percent for this task and consequently it is just an adaptation of our photometric bench presented elsewhere. It could be roughly described, as its photometric counterpart, as a «direct illumination LED calibration».¹

The results that we present here go much beyond owing to the great intrinsic stability of the LED source and of our electronics. We shall use them to illustrate the concepts of calibrated LED source and of spectrophotometric calibration bench. In our opinion these results opens seriously the discussion of a new line of photometric standards reaching much smaller intensities and much higher precision than those on the market.

For some applications the calibrated light sources might replace advantageously calibrated detectors.

¹ In fact the spectrometer grating is illuminated either directly or through two auxiliary mirrors and the first order reflecting beam never overlaps beams of other orders owing to the limited LED bandwidth.

2 Description of SNDICE spectral bench

Figure 1 gives an overview of SNDICE's spectral calibration bench. The detailed

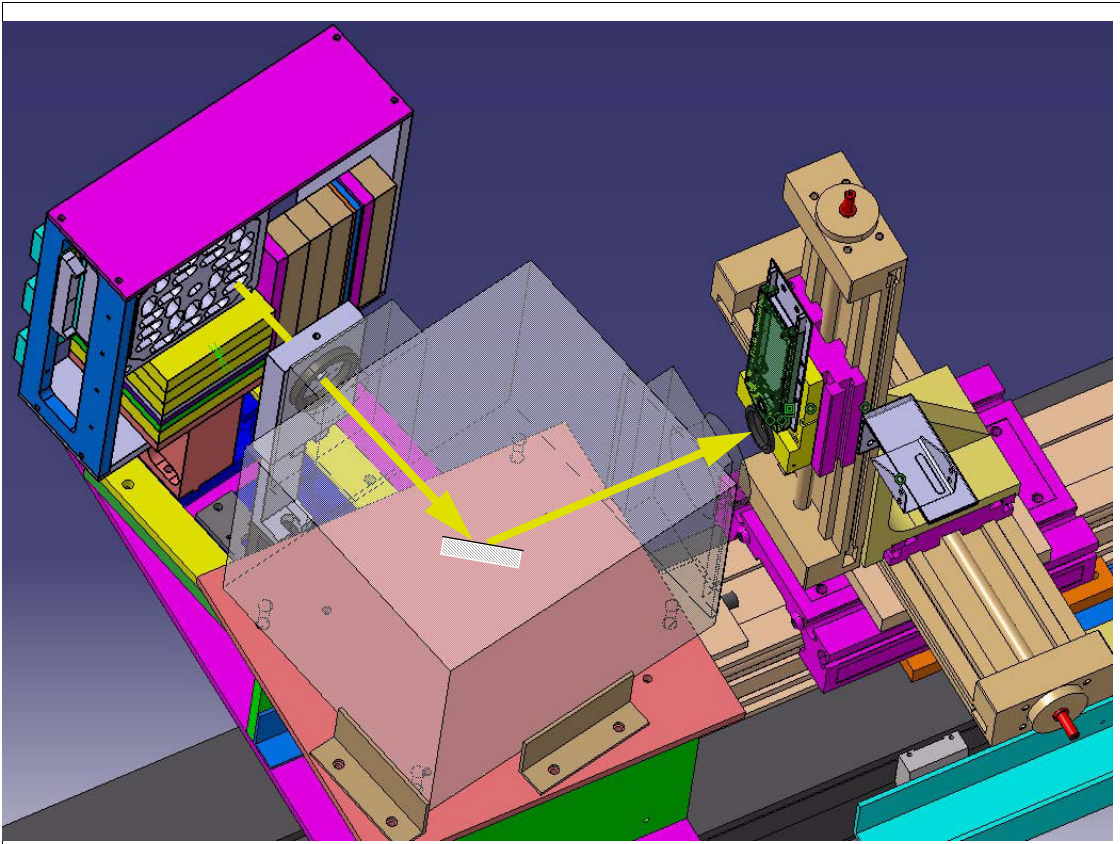


Figure 1: View of the SNDICE spectral calibration setup drawn by realistic rendering option of CATIA CAD. Yellow arrows materialize the LED light beam from a channel in the LED-head (upper left) to the calibrated photodiode mounted on a XYZ motion (center right) through a shutter and a monochromator (represented by a translucent box around a grating symbolized by a cross-hatched rectangle). The LED-head is configured «short», i.e. using only one out of eight longitudinal segments (cf. Figure 2). Two orthogonal piles of wedges are used to position the LED-head horizontally and vertically inside a frame (top left) so that each LED can be centered within 1/3 mm on the optical axis of the bench. The whole setup is mounted on a 2.5 m granite bench. Several other detectors can be mounted on the XY stage above the calibrated detector, to be compared with it.

structure of the LED source is shown in Figure 2. The LED spectra are measured around the optical axis of the source. They are assumed not to depend on the exact position of the detector within the field. The detector, the electronic and the data acquisition setup of the spectral calibration bench are identical to those of the photometry bench.

The setup of the calibration bench is shown in Figure 3. The LED source mounts are different for the photometric and the spectral versions of the bench, in order to accommodate for the reflection of the optical axis by the monochromator grating and its two collimating mirrors (100° overall angle). The light beam is sufficiently narrow in the spectral case to be entirely contained within the detector, as shown in Figure 4. It is defined by the LED dice, the entrance and exit slits of the monochromator, all being

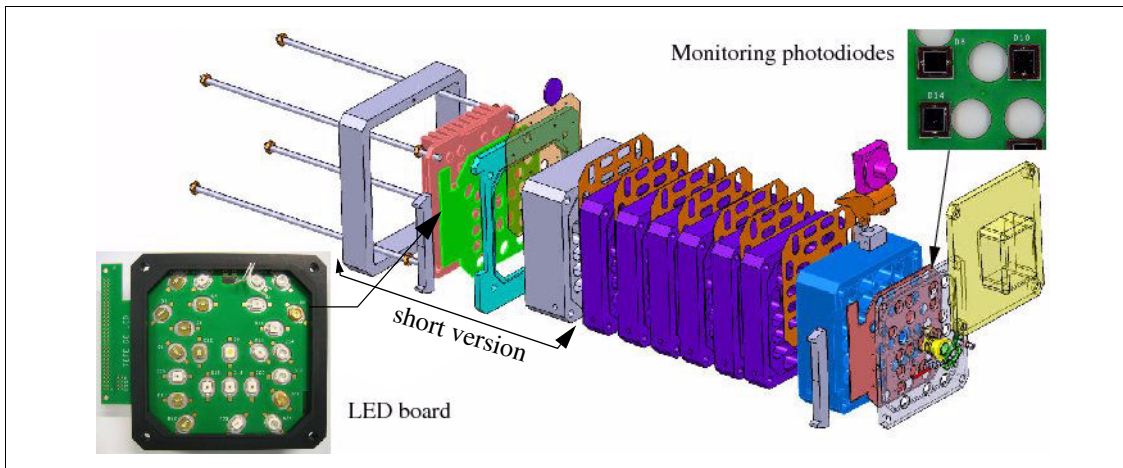


Figure 2: Exploded view of SNDICE LED light source. The «long» version includes the eight segments (in blue) perforated by 25 holes which define 24 calibrated LED light beams (1.5° conical) plus one artificial planet beam ($\varnothing 1\text{cm}$ cylindrical and white). The «short» version, with a single segment, uses the entrance slit of the monochromator as the beam defining aperture.

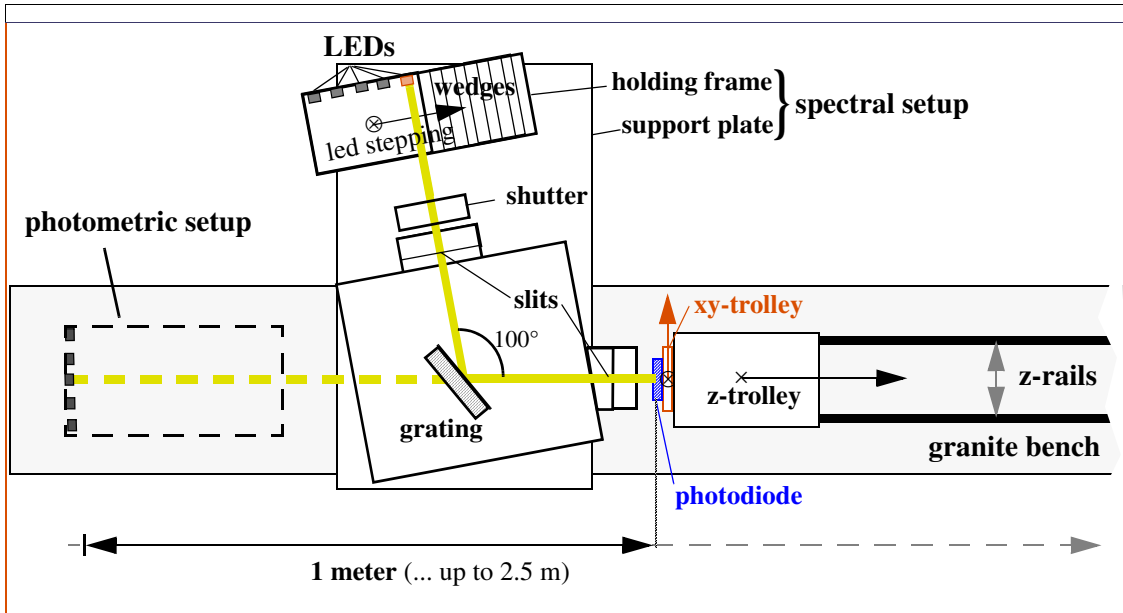


Figure 3: Top view of the calibration bench spectral setup drawn in Figure 1. The position of the long LED source and its light beam in the photometric setup are figured in broken lines.

approximately 0.3 mm wide in the horizontal plane.

The detector alignment is done automatically using the x-y motion to scan the beam as shown in Figure 4 . The y (vertical) motion is also used to alternate data taking with different detectors on a common monochromatic light beam, for instance to cross-calibrate them. The monochromator is a Czerny-Turner (TRIAx-180 from Jobin-Yvon Horiba). It provides 3 interchangeable gratings and the average wavelength and the width of slits are programmable.

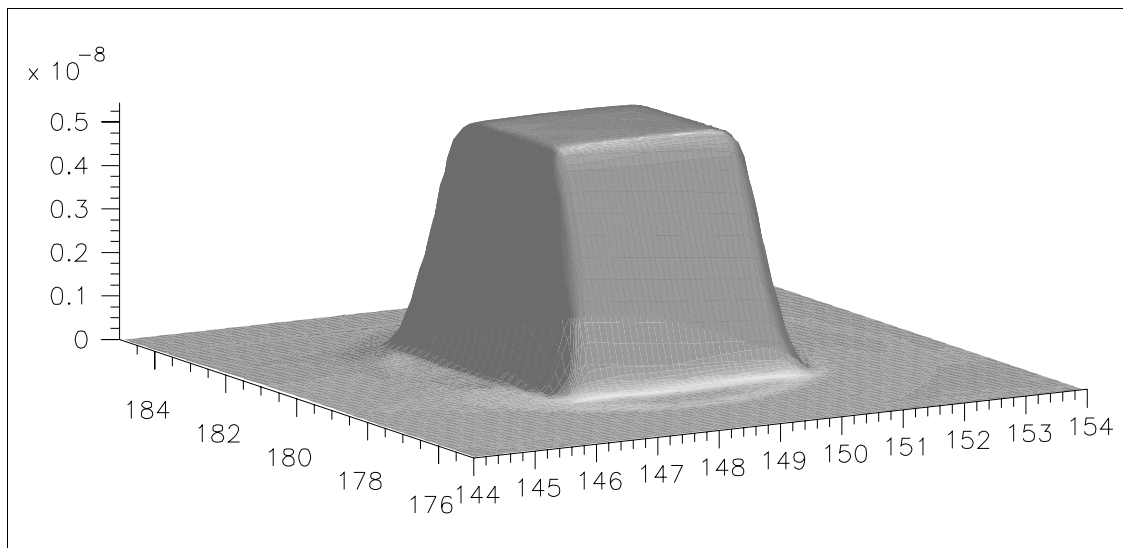


Figure 4: X-Y (cm) scan of the monochromator beam with the CLAP detector; z is photocurrent (A).

3 Spectral model of SNDICE light flux

SNDICE is used mainly to measure the photometric response of a telescope system illuminated by 24 LEDs. These 24 responses are obtained by the convolution of the telescope model with the LED spectra. The first role of the SNDICE spectral bench is to measure these spectra. They can be described either as a peaked curve or by a model depending on a few parameters. Our model, shown in Figure 5, consists of five third-degree polynomial approximations covering five characteristic regions: the peak region, the rise ('blue' edge) and the fall ('red' edge) around the peak, and the blue and red tails. The intuitive meaning of these parameters is essentially the position and width of the peak, the position and the slope of rising and falling edges, and the asymptotic description of the tails.

For example, in the GD8 example (Figure 5), for a rise (or a fall) of half of the peak, the wavelength step is 9 nm (or 6 nm). These numbers depend on the LED considered but their orders of magnitude are the same.

The tails tend asymptotically towards a stray light flux ($\sim 10^{-3}$ of the peak value and stable), while dark current and single measurement precision are kept below 10^{-4} . The approximation error of our polynomial fits being larger than the measurement precision, for some applications we will rather use directly the spectral calibration curve.

4 Coarse grained versus fine grained spectral resolution of SNDICE

A second use of the SNDICE spectral bench is to calibrate our CLAP detector (or any other device) by comparison with a NIST calibrated photodiode. It provides a fine grained resolution to complement the coarse grained resolution of the photometric bench. This bench (cf. C. Juramy report) yields a stable and precise (10^{-4} ?) 3-d mapping of the radiation field produced by the 24 LEDs (detector surface being perpendicular to

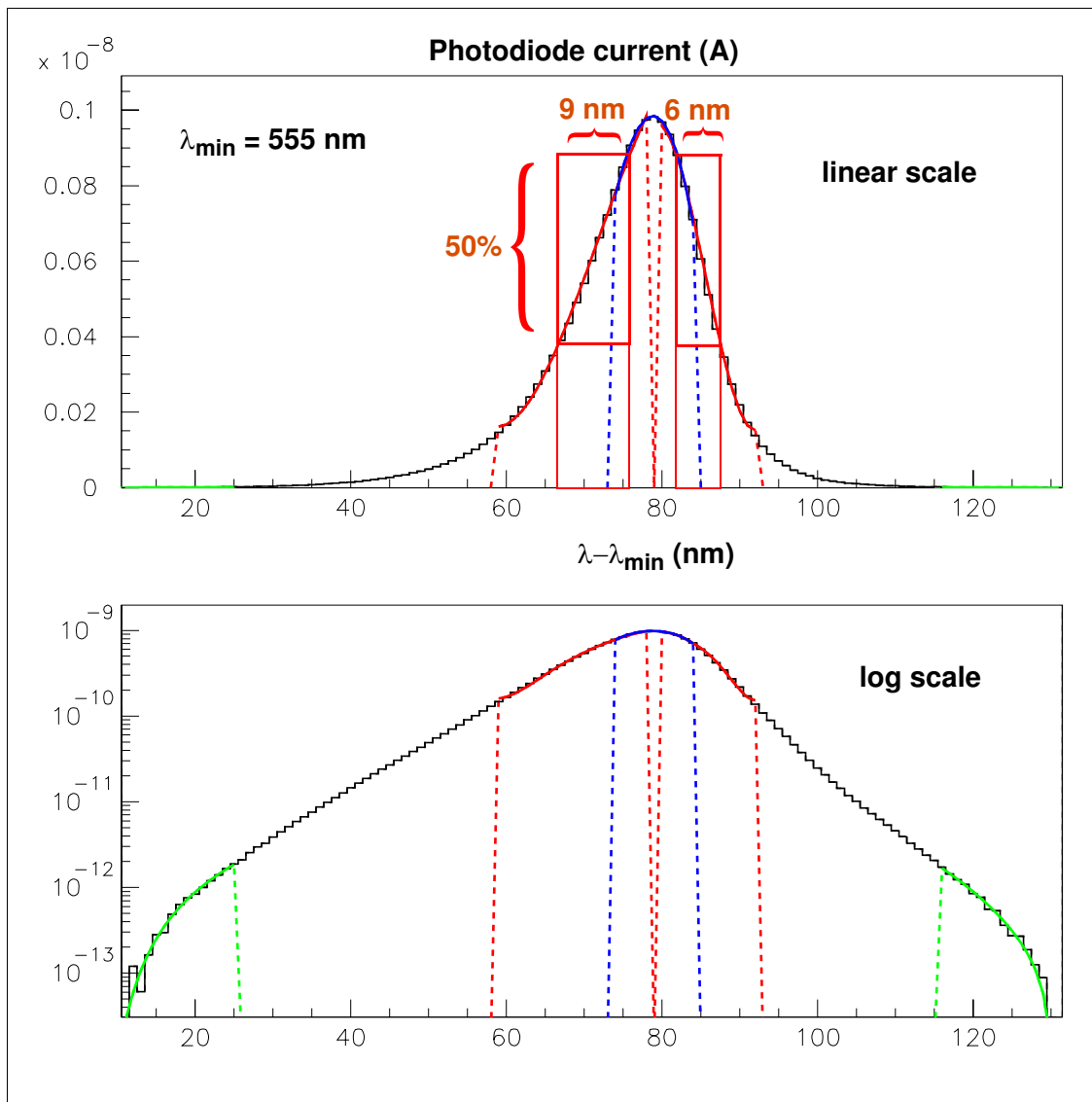


Figure 5: Empirical fit of a led spectrum subdivided in five regions peak (blue) rise and fall (red) and tails (green) in which spectrum is reproduced by a third degree polynomial. The led here is a Golden-Dragon (GD8)

the SNDICE axis). Each reading is understood as proportional to the effective surface of the photodiode, to the quantum efficiency (QE) averaged over the spectral distribution of the LED and to the current traversing the LED. The comparison of two detectors using the spectral bench will yield as in Figure 6 a whole set of relative quantum efficiencies per LED.

The main weakness of the spectral setup is the commutation of the LED channels needed to scan the whole range of wavelength from near IR to near UV. The electronic commutation is simple and fast, but the LED's exchange has not been motorized. The reproducibility of the monochromator beam implies that the center of a LED replacing another comes exactly on the same point on the optical axis of the monochromator. The displacement of the LED head is realized by shifting a few wedges from one side of the head to the other. The lack of precision of this operation limits the reproducibility of

spectral measurements across the whole spectrum. Figure 6 shows that it is comprised in

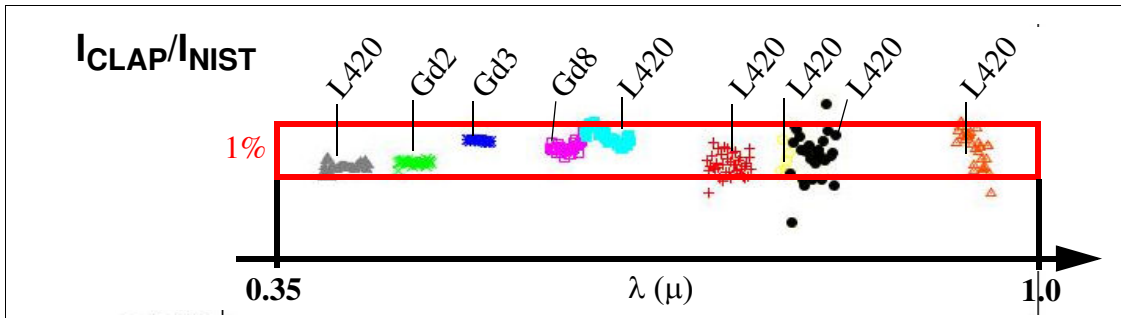


Figure 6: Ratio I_{CLAP}/I_{NIST} of the responses of two photodiodes as a function of wavelength for 9 out of 24 LEDs (from A.Guyonnet, Rapport de Stage M2, June 2009). A bias ($\pm 0.5\%$) mainly due to bad centering of the monochromator beam occurs on some data. This effect is below 10^{-3} for well centered thermalized photodiodes such as GDxx (left). (CLAP and INIST diodes have very similar QE explaining the flat band).

a $\pm 0.5\%$ band in this test but that it could be below 10^{-3} with a better positioning as tested for a few LEDs. Therefore an automatic positioning of the short LED source is required for transforming the SNDICE spectral bench into a spectrophotometric detector calibration device. We shall see that most other requirements -essentially linearity, stability and reproducibility- are fulfilled down to the 10^{-4} level after some adjustments concerning temperature dependence of LED spectra and angular dependence of LED emission.

5 Limiting precision of the spectral bench and related temperature effects

The limiting precision of the spectral bench is around 10^{-4} . This number expresses the stability and the reproducibility during 7 consecutive days of the current measurement in one of the photodiodes after many measurement cycles involving wavelength scans and detector exchanges.

Stability is tested by a chain involving the light source and its electronics in one side and a light detector and its electronics on the other side. This makes four components in the chain. Any one of them could drift. The stability achieved is limited by the less stable element. In our setup the electronics controlling the LED source is tested independently of the emission of light. Actually the electric current flowing through the LED is monitored. Its stability is shown to be $\approx 0.5 \times 10^{-4}$ (see Figure 7 a). We used in this test the reference detector of our photometry calibration bench, because our ultimate aim is to calibrate the light source rather than to test its stability. This is a NIST calibrated photodiode (or another DKD calibrated photodiode) read out by a Keithley picoammeter. They turned out to be the less stable than the LED. We attribute this point to the photovoltaic readout mode chosen by NIST, which deserves a special discussion (cf. A.Guyonnet) and justifies the development of the CLAP² (which is the detector side of

² "Test of a Low Current Amplifier ASIC for Cooled Large Area Photodiodes"; E.Barrelet, LPNHE 2007-04

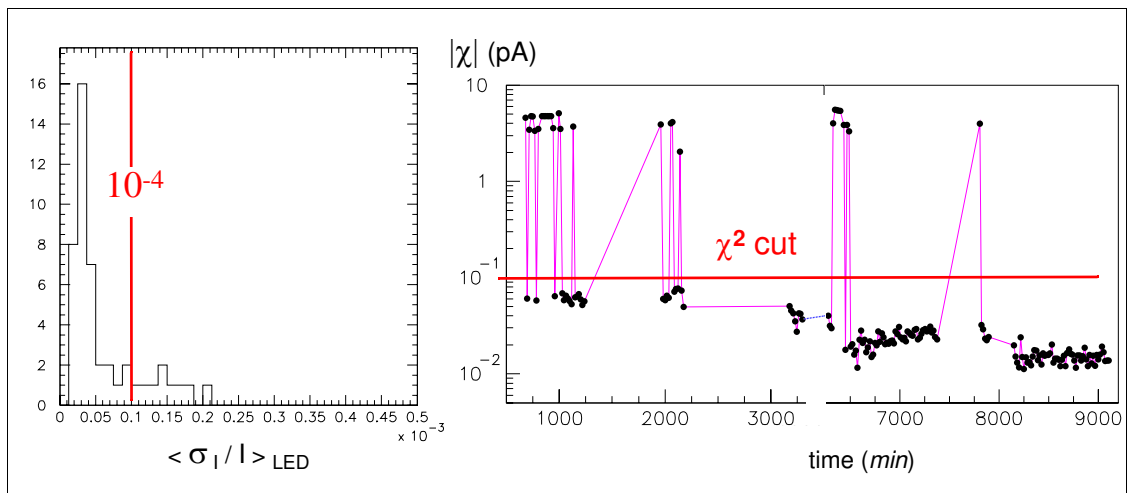


Figure 7: a) Relative fluctuation of the LED current (I_{LED}); b) Rejection of periods of instability of the photometric signal using an empirical statistical cut on I_{zp} ($|\chi| > 10^{-1}$ pA)

the SNDICE project). But our photodetector problem has been overcome using two tricks described hereafter.

5.1 Stabilisation of the current readout

We measure a dark current which should be null according to p-n junction theory (and common sense). Therefore we prefer to call it “Zero Point Current”³ (ZPC). We observe erratic jumps of ZPC (± 5 pA) between quiet periods, sometimes occurring after a reset of the picoammeter. The periods of instability are suppressed using an empirical χ^2 test. The fluctuation of this «instability χ^2 » during the run is shown in Figure 7b). In addition to these jumps there is an overall temperature dependence of the ZPC. Data from the stability run are partitioned in five periods corresponding to five average room temperatures in a 3°C range and one period is chosen as a reference. The differences of the spectral distribution of LED light between the reference period and the others is shown in Figure 8. This partition of the stability run in five allows to eliminate the mean effect of thermal as well as ZPC fluctuations. The RMS fluctuations during the whole 7 days are shown in Figure 9, before partition (in blue) and after (in red).

They tell that in a room environment with a temperature excursion of 3°C LED a simple spectral model is valid within 0.25% and the corresponding photometric stability is within 0.15% (because when integrating the flux on the whole spectrum red and blue sidebands compensate each other). When taking into account the effect of LED temperature on spectrum by steps of 0.5°C the stability goes to a better than 5×10^{-4} level. Actually the RMS fluctuations at this level came in this test essentially from statistical photon noise (“Poisson”) and from ADC quantification noise which can be lowered with better data taking conditions.

The specific study in Section 5.2 of the temperature effect using the temperature gauge within the LED source to implement a correction at a 0.1°C level brings a spectral

³ Keithley’s photocurrent extrapolated at zero light flux

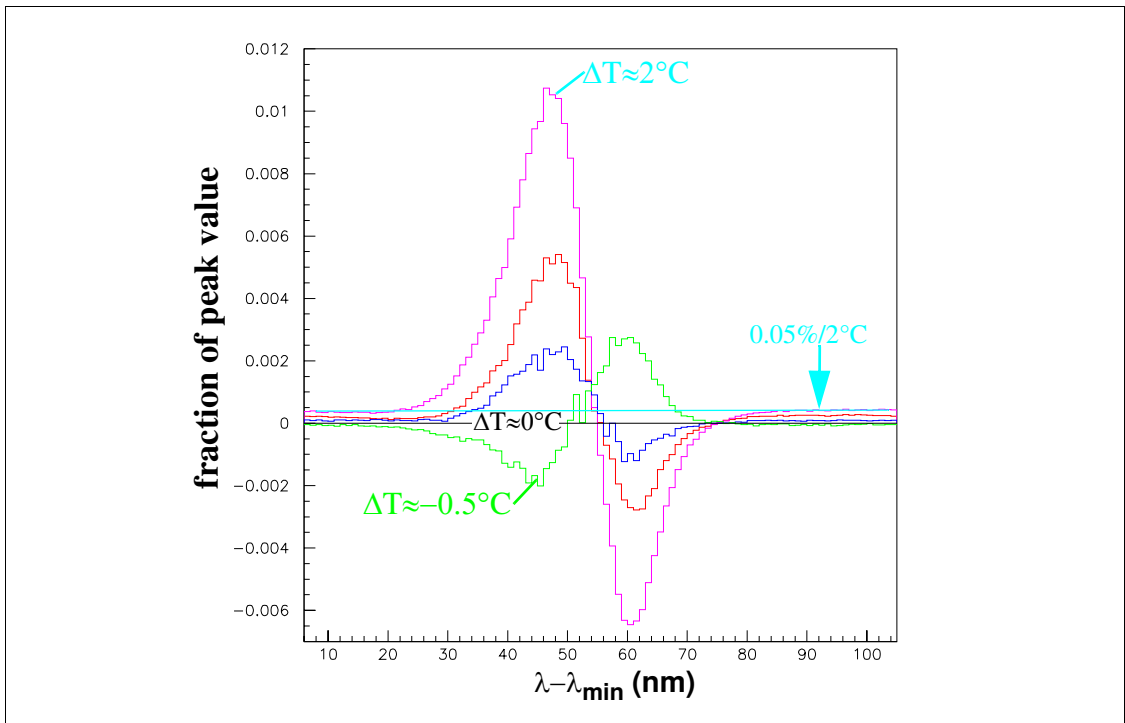


Figure 8: Difference of average spectra taken at different periods of the stability run. The tails of the spectra are consistent with a residual dark current component $\approx 2.5 \times 10^{-4}/^{\circ}\text{C}$.

stability of 10^{-4} . There is a good indication that with a thermalization of the LED at 0.1°C one would observe a stability and a reproducibility better than 10^{-4} . This is not achievable with other light sources but this result does not take into account aging effects (monochromator mirrors, etc...).

5.2 The thermal shift of LED spectra

Practically this study was done by installing an air-conditioning device inside the dark cabinet enclosing the calibration bench. The temperature could be adjusted between 16° and 24°C . The probe fixed inside the LED head gave the LED temperature.

The modification of the spectrum $S(\lambda, T)$ with varying temperature is encoded by an empirical discrepancy function:

$$\delta S(\lambda, T) = S(\lambda, T + \delta T) - S(\lambda, T) \sim \Delta S(\lambda) * \delta T$$

These discrepancy functions for the LED GD8 are represented in Figure 10. The crossing point at $\lambda - \lambda_{\min} = 80 \text{ nm}$ is due to the combined effect of a slide toward the red and an increase of amplitude with increasing temperature (This is not the case for all LEDs).

From these discrepancy functions, we have extracted in Figure 11 the best estimate for the LED temperature effect. We have correlated three estimators: a red and a blue edge shift estimator (either the maximum or the minimum of the discrepancy function) and a temperature monitor computed by averaging the measurement of a platinum resistor glued on the metal plate on which all LEDs are fixed.

The correlation between red and blue edges is shown in Figure 11. It yields a 2.5×10^{-4}

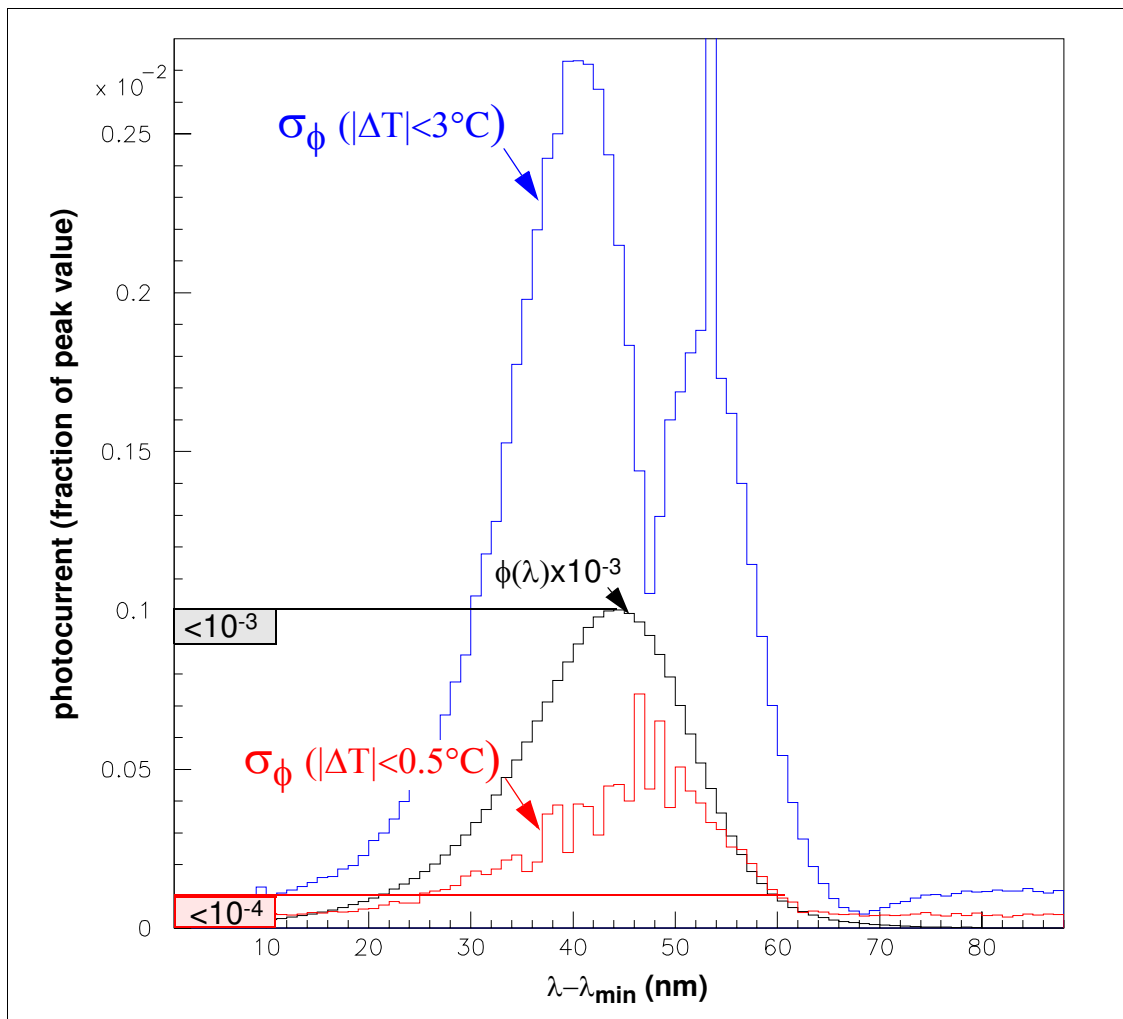


Figure 9: RMS fluctuation of the photocurrent as a function of wavelength: in **blue** globally during seven days ($\Delta T < 3^{\circ}\text{C}$); in **red** restricted to a set of periods of moderate temperature variation as shown in Figure 8 ($\Delta T < 0.5^{\circ}\text{C}$). For comparison in **black** the spectral distribution of the light flux normalized to one per mil (symbolic stability thresholds of 10^{-3} and 10^{-4} are indicated with horizontal lines).

RMS which we took as the measurement of the stability of our bench. The correlation between both edge estimators and the temperature monitor yields a 4×10^{-4} RMS. This could result of a slightly different temperature ($\sim 0.01^{\circ}\text{C}$) between the monitor Pt resistor and the LED.

The 2.5×10^{-4} photocurrent precision, when taking into account the slopes of red and blue edges translates respectively into a 5 pm and 3 pm precision on the mean wavelength characterizing both edges. Looking at orders of magnitude we cannot tell yet what part of the temperature effect seen on the spectra come from the LED and what part come from the spectrometer.

It is impossible to do better with the present temperature control which keeps temperature varying during the acquisition of a spectrum and which do not discriminate between effects affecting one subsystem or another, but at least we can exclude perturbations other than temperature at the 10^{-4} level.

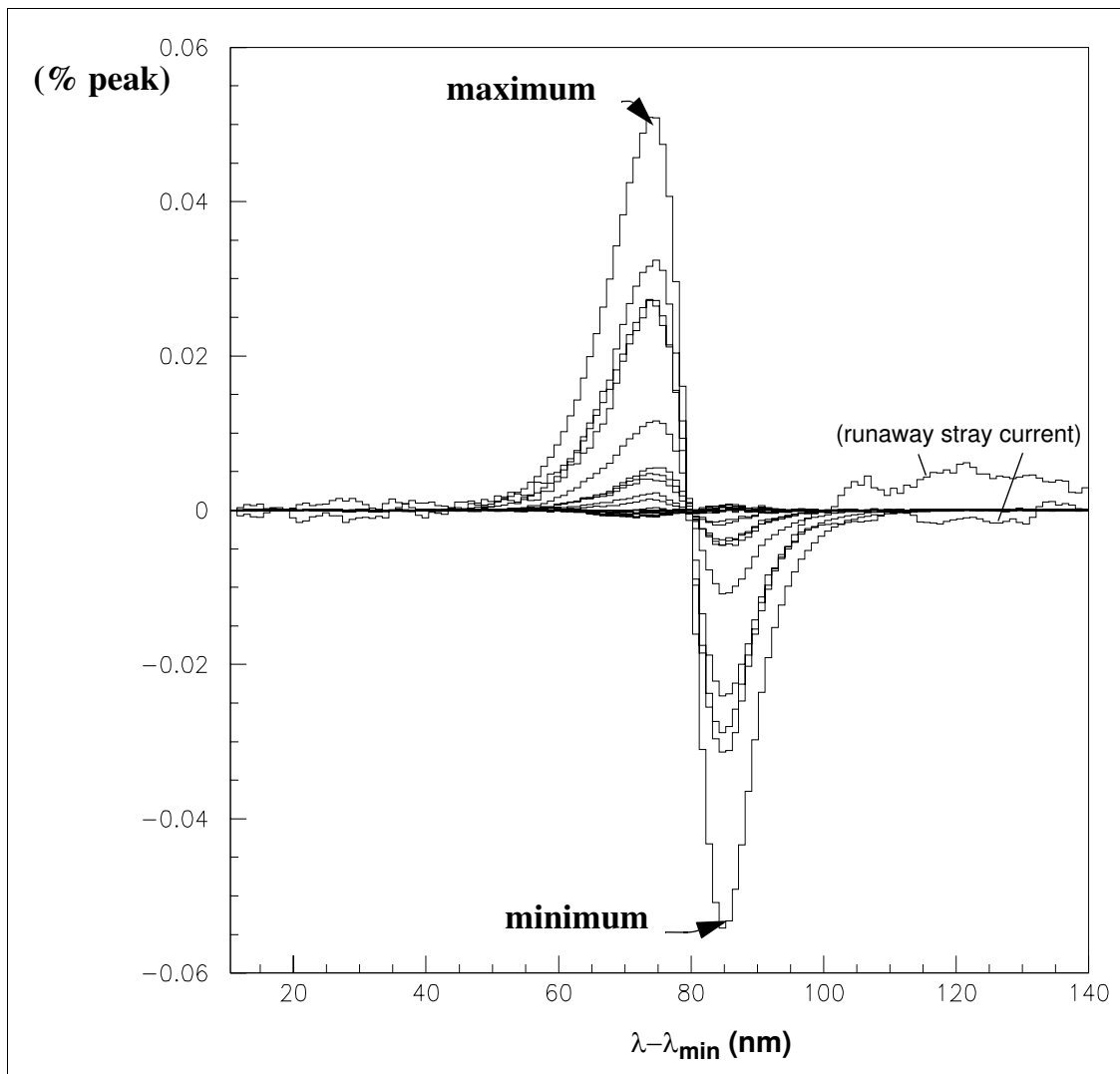


Figure 10: Discrepancy functions representing the effect of varying LED temperature on the Gd8 LED spectrum as the difference between the two spectra taken at different temperature. Maxima and minima are plotted in Figure 11. (Two spectra present runaway stray currents affecting essentially the red tail)

6 Conclusions

The primary task of our spectral calibration bench is to provide us with a reference spectrum for each LED. This is a necessary complement to the photometric calibration of the LED source obtained with the same calibration bench. It is needed to compute the effect of the spectral spread of a LED beam on a given photometric response (either a detector quantum efficiency or a filter transmission) as a second order correction of the raw photometric estimate.

Moreover our study has found that our bench presents an exceptional precision of $\sim 10^{-4}$. This number represents the reproducibility of our measurements on a week timescale

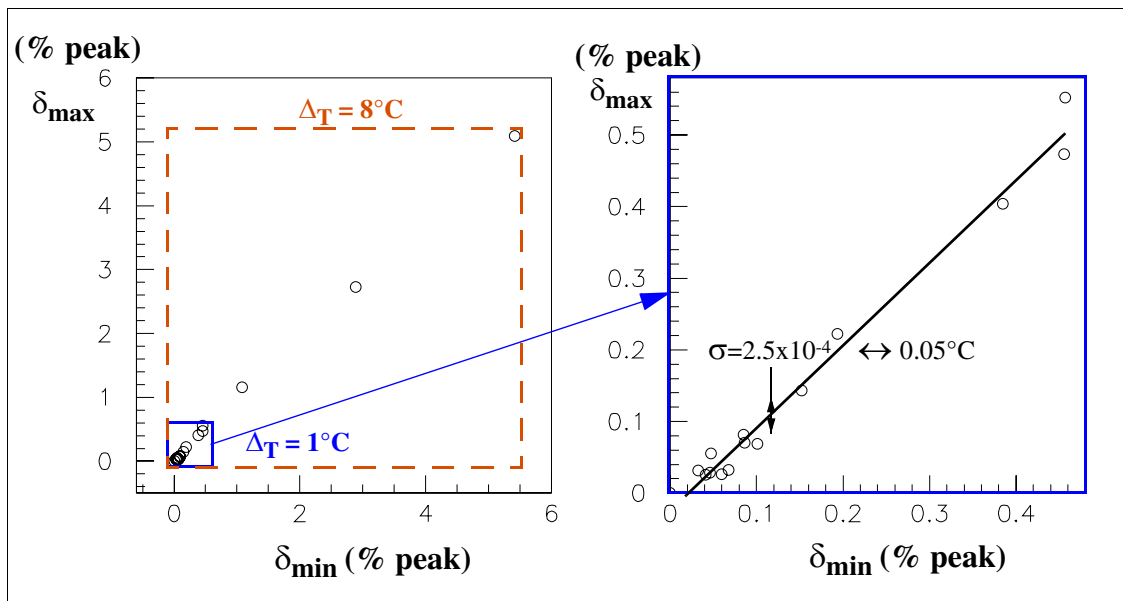


Figure 11: Maximum vs Minimum discrepancy between any spectrum ($16^\circ < T < 25^\circ$) and the reference spectrum ($T = 16^\circ$) for a given led (Gd8). These extremes discrepancies are varying linearly with temperature, with a slope of 0.65% of peak value per degree. These figures are compatible with a reasonable stability of room temperature $\sim 3^\circ\text{C}$ during the 7 days test.

when temperature is controlled at a $< 0.1^\circ\text{C}$ level. The same study shows that the temperature dependence of a LED spectrum is easily modeled and measured with our bench, and that it can be used to predict or to measure the effect of temperature on a photometric measurement at the same ($\sim 10^{-4}$) level of precision. This analysis is complicated by the instability of the photodiode readout in the photovoltaic mode. The spectral bench operation is very different from a spectrophotometric absolute calibration, provided by calibration institutes at a much cruder level (by 2.5 order of magnitude).

We have analysed the calibration data from the SNDICE LED light source which had been obtained rapidly before sending it to CFH in Hawaii. Then we performed a detailed analysis of the temperature effect using our spare SNDICE system. It remains to fully automatize our calibration bench. This is essentially a software project which could be developed on the spare SNDICE system. It should integrate photometric and spectral calibration benches and include a critical study of the work done by calibration institutes on our reference detectors.